Electronic Supplementary Information

Core-Shell Noble-Metal@Zeolitic-Imidazolate-Framework Nanocarriers with High Cancer Treatment Efficiency *in Vitro*

Liangcan He,‡[a] Kanglei Pang,‡[abc] Wenwen Liu,[a] Yue Tian,[a] Lin Chang,[a] Xu Liu,[a] Meiting Zhao,[a] Yong Liu,[a] Yantao Li,[a] Xingyu Jiang,[a] Rui Song*[b] and Yaling Liu*[a]

[a] *CAS Key Laboratory of Nanosystem and Hierarchical Fabrication, CAS Center for Excellence in Nanoscience, National Center for Nanoscience and Technology, No.11, Beiyitiao, Zhongguancun, Beijing 100190, P. R. China. *E-mail: liuyl@nanoctr.cn*

[b] *School of Chemical Sciences, University of Chinese Academy of Sciences, No.19, Yuquan Road, Shijingshan District, No.19, Yuquan Road, Shijingshan District,Beijing 100049, P. R. China. *E-mail: rsong@ucas.ac.cn*

[c] *Sino-Danish College, University of Chinese Academy of Sciences, No.19, Yuquan Road, Shijingshan District, Beijing 100049, P. R. China.*

† Electronic Supplementary Information (ESI) available. See DOI: 10.1039/x0xx0000x.

‡ These authors contributed equally to this work.

Part SI: Detailed Materials and Methods.

Materials: Tetrachloroauric acid ($HAuCl_4$) and poly-vinylpyrrolidone (PVP, M.W. 30000) were purchased from Sinopharm Company. N,N-dimethylformamide (DMF) was bought from Beijing Chemical Works. Zinc nitrate hexahydrate ($Zn(NO_3)_2{\cdot}6H_2O$) and 2-methylimidazole were provided by Alfa Aesar. Doxorubicin hydrochloride (DOX) was purchased from Beijing Huafeng United Technology Co., Ltd. Cell Counting Kit-8 (CCK-8) was bought from Dojindo Laboratories (Japan). All the chemicals were used as received. HeLa cells were obtained from the American Type Culture Collection (ATCC). Ultrapure water (Millipore Milli-Q grade) with a resistivity of 18.2 MΩ was used in all the experiments. Calcein-AM and Propodium iodide were bought from Shanghai Yisheng Biological Technology Co., Ltd.

Preparation of the core-shell Au@ZIF-8 nanostructures: 0.01451 g $Zn(NO_3)_2{\cdot}6H_2O$, 0.00364 g 2-methylimidazole and 0.1456 g PVP were dissolved in 8 mL DMF solution in a 15 mL autoclave. After dissolving thoroughly, 20 μL $HAuCl_4$ solution that was pre-prepared by dissolving 1 g $HAuCl_4$ in 40 mL pure water was added into the autoclave. Then, the autoclave was transferred to an oven with a constant temperature of 140°C. After 4 h reaction, the solution became blue grey, and blue grey products were obtained via centrifugation at 3500 rpm for 8 min. The products were washed with DMF for several times by centrifugation at 3500 rpm. Subsequently, the products were dispersed into $CHCl_3$ for 12 h for three times in order to remove residual DMF by centrifugation. Finally, the products were dried in vacuum at 150°C for 24 h for further characterization and experiments.

Characterization: Transmission electron microscopy (TEM) images were carried out using Tecnai G2 20 S-TWIN at 200 kV. High angle annular dark field scanning transmission electron microscope (HAADF-STEM) imaging and energy dispersive X-ray spectrometry (EDX) elemental mapping were performed by FEI Tecnai G2 F20 S-TWIN at 200 kV. Powder X-Ray diffraction (XRD) patterns were recorded on

D/MAX-TTRIII (CBO) with Cu Kα radiation (λ = 1.542 Å) operating at 50 kV and 300 mA. UV-Vis absorption spectra were obtained with U-3010 spectrophotometer (Hitachi). A He-Ne laser (514 nm) was used as the light source for exciting the core-shell nanostructures. The laser power in the release experiment was 50 mW, and the radius of the laser light source was 0.5 μm. The HeLa cells were irradiated with the M-visual light source (wavelength: 400~700 nm, MVL-210, MEJIRO GENOSSEN, Japan) at 20 $mW \cdot cm^{-2}$. Images were acquired using FV 1000-IX81 confocal laser scanning microscope (Olympus, Japan).

DOX loading into core-shell Au@ZIF-8 nanostructures: The core-shell Au@ZIF-8 nanostructures and the DOX powder were mixed in aqueous solution at various concentrations (Table S1). After that, the mixture solution was stirred in dark at room temperature. After 4 days, the DOX-loaded Au@ZIF-8 (Au@ZIF-8-DOX) complex was produced and then collected by centrifugation at 10000 rpm for 10 min. Furthermore, the products were washed for five times with pure water to remove the physically adsorbed DOX molecules. Notably, the amount of DOX loaded in the core-shell Au@ZIF-8 nanostructures was determined using UV-Vis spectroscopy at 480 nm.

DOX *in vitro* release from the Au@ZIF-8-DOX complexes: In the *in vitro* drug release experiments, 0.5 mL Au@ZIF-8-DOX buffer solution of a certain pH value (6.0 or 7.4) was agitated at 37 °C. The mixture was centrifuged at half an hour intervals. The supernatant liquid was collected and the same volume of fresh buffer was added back to the residual mixture. The amount of the released DOX in the supernatant solution was determined by UV-Vis spectroscopy at 480 nm. In the laser irradiation experiments, a similar procedure was performed and the Au@ZIF-8-DOX solutions were irradiated with a laser (wavelength, 514 nm; beam diameter, 1.0 μm; power, 50 mW).

Cell culture and treatment: The HeLa cells were cultured with Dulbecco's modified Eagle medium (DMEM) (Invitrogen, USA) supplemented with 10% fetal bovine serum

(Hyclone Company, South Logan, UT), penicillin (100 μg·mL^{-1}), and streptomycin (100 μg·mL^{-1}, Gibco, Grand Island, NY, USA) in 5% CO_2 at 37°C in a humidified incubator. After cultured in 96-well plates for 24 h, the HeLa cells were incubated with different materials (DOX, Au@ZIF-8 or Au@ZIF-8-DOX) for 3 h at 37 °C in the dark. After removing the culture medium, the DMEM was added into the plates. The incubated HeLa cells were provided for irradiation experiments, and the cell viability was observed using confocal fluorescence microscope with green color for live cells and red color for dead cells.

Detection of the photodamage of intracellular organelles by fluorescent probes: Immediately after irradiation, control or PDT-treated cells were incubated with DMEM containing FM4-64, BODIPY®TR Ceramide complexed to BSA and Lyso-Tracker Green at 37°C as recommended by the manufacturer (Invitrogen). Then, the cells were rinsed with DMEM and used for detection of the integrity of the cell lysosomal membranes by observing the dye distribution by confocal microscopy. Images were acquired using FV 1000-IX81 confocal laser scanning microscope (Olympus, Japan).

Cell viability assay: For the dark cytotoxicity examination, cells were cultured with different materials for 24 h at 37°C in the dark. Cell viability was evaluated using a WST-8 assay with a Cell Counting Kit-8 (CCK-8; DOJINDO, Kumamoto, Japan). The absorption value at 450 nm was read with a 96-well plate reader (iMark microplate reader, Bio-RAD, USA) to determine the viability (cell viability = $(OD_{tre}-OD_{medium})/(OD_{con}-OD_{medium})$), where OD_{tre} was the absorption intensity at 450 nm of the treated cells, OD_{con} was that of control cells and OD_{medium} was that of the culture medium.

Cell apoptosis assay: After cultured in 12-well plates for 24 h, the HeLa cells were incubated with different materials (DOX, Au@ZIF-8 or Au@ZIF-8-DOX) for 3 h at 37°C in the dark. After removing the culture medium, the DMEM was added into the

plates, HeLa cells were irradiated by a 20 $mW \cdot cm^{-2}$ light with the wavelength of 400 - 700 nm for 0 and 30 minutes, respectively. After cultivated for 24 h at 37°C in the dark, cells were washed two times with PBS after trypsinization. Subsequently, live and dead cells were fluorescently labeled with the cell stains Calcein-AM and Propodium iodide and resuspended in Hank's Balanced Salt Solution (HBSS). The apoptosis rate of HeLa cells was determined by flow cytometry.

Cellular Uptake of DOX: For the cellular uptake of DOX examination, HeLa cells were seeded in a 6-well plate and incubated overnight, and then HeLa cells were cultured with 10 μM DOX and equivalent dose of Au@ZIF-8-DOX for 1, 3, 6, and 12 h, respectively. After trypsinization, cell were washed two times with PBS and resuspended in Hank's Balanced Salt Solution (HBSS), then the internalized amount of DOX and Au@ZIF-8-DOX was quantified by flow cytometry due to the strong fluorescence emission around 580 nm and the wide absorption spectroscopy around 480 nm of DOX.

Part SII: Structural characterization of core-shell Au@ZIF-8 nanostructures and their drug delivery properties.

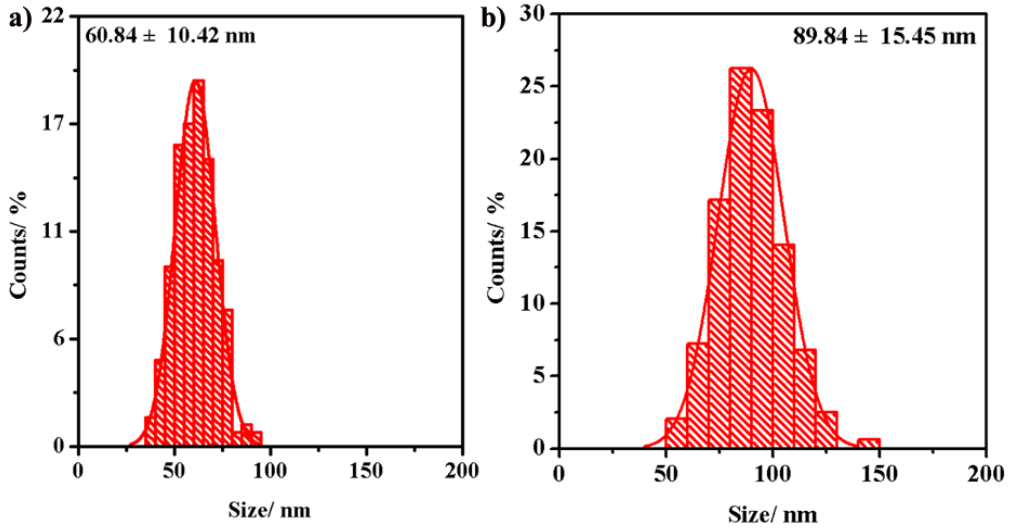

Fig. S1 Statistic data of (a) the cores and (b) the shells of the core-shell Au@ZIF-8 nanostructures.

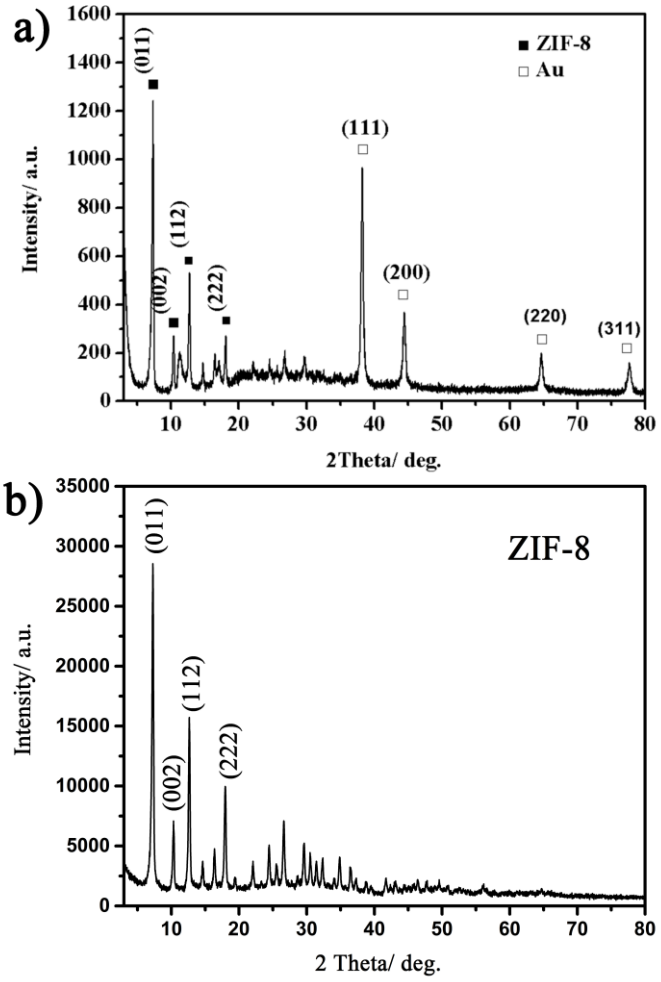

Fig. S2 Powder X-ray diffraction (XRD) pattern of a) core-shell Au@ZIF-8 nanostructures and b) pure ZIF-8.

Powder XRD pattern confirms that these nanostructures are composed of two components, face-centered cubic Au and cubic crystalline ZIF-8, and no peak assigned to other impurities is detected.

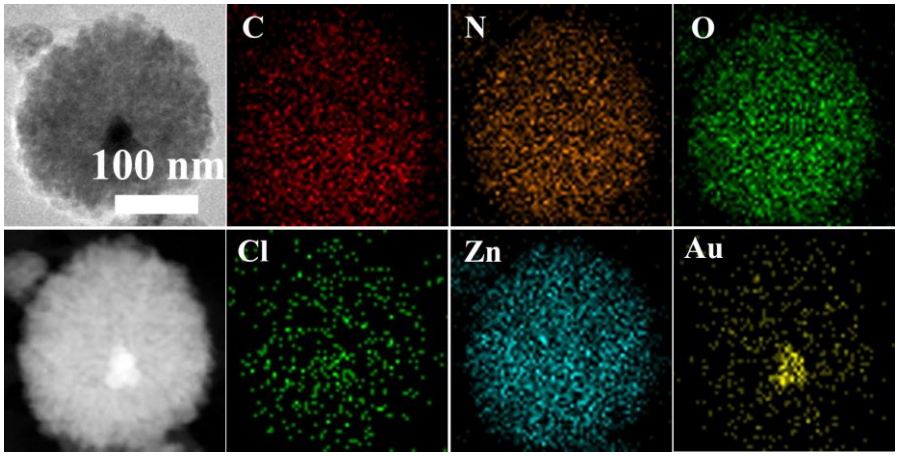

Fig. S3 EDX elemental mapping of a core-shell Au@ZIF-8 nanostructure after DOX loading.

It is known that among all the three components of the Au NP cores, the ZIF-8 shells and the loading DOX in the core-shell nanostructures, only DOX contain the element O and Cl (the molecular structure of DOX is shown in the below). So, uniform distribution of the element O and Cl as shown in Fig. S3 highlights the homogenous loading of DOX into the whole core-shell Au@ZIF-8 nanostructures.

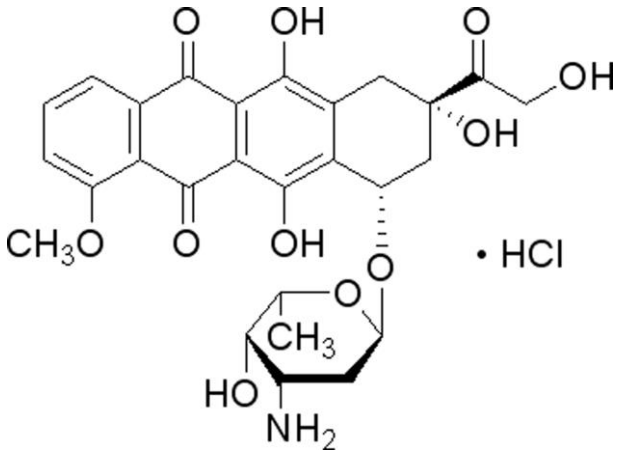

The molecular structure of DOX

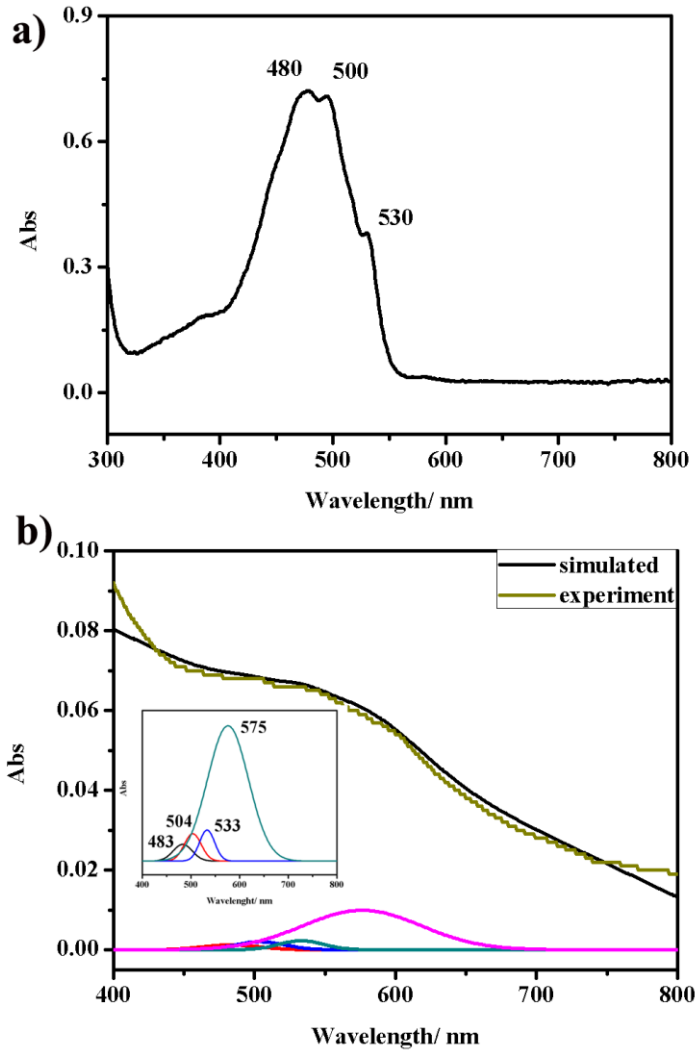

Fig. S4 (a) UV-Vis spectrum of DOX in aqueous solution. (b) Peak processing of the magnified UV-Vis spectrum of the Au@ZIF-8-DOX complexes shown in Fig. 1b by the peakfit software.

The broad peak between 400 nm and 600 nm is overlapped by 4 different peaks, which is illustrated in Fig. S4b. The peaks at 483, 504 and 533 nm can be ascribed to the DOX molecules, and the peak at 575 nm is attributed to the gold nanoparticles. The slight red shift of peaks of DOX is mainly due to the interaction between DOX and the Au@ZIF-8 nanostructures.

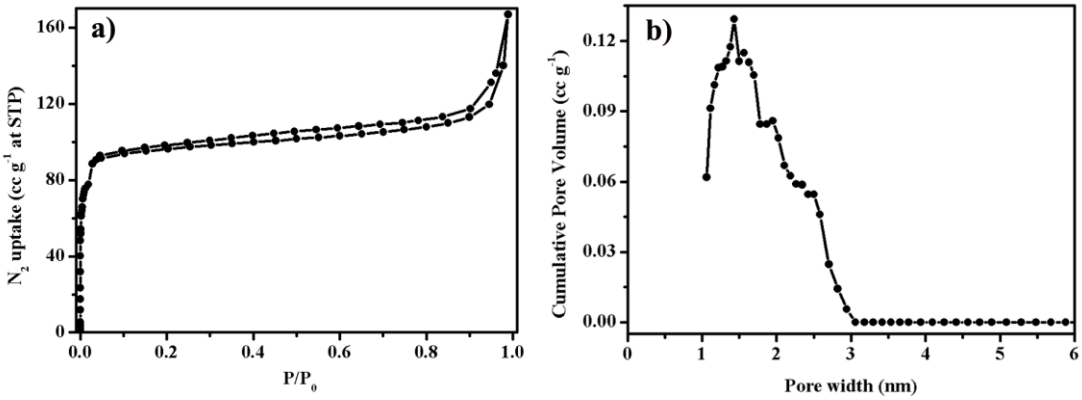

Fig. S5 (a) N_2 adsorption-desorption isotherms of core-shell Au@ZIF-8 nanostructures. (b) Pore size distributions calculated by the non-local density functional theory (NLDFT) method for core-shell Au@ZIF-8 nanostructures.

The surface area of the core-shell nanostructures is 422.25 $m^2 \cdot g^{-1}$. The pore width is 1.43 nm and the pore volume is 0.17 $cc \cdot g^{-1}$.

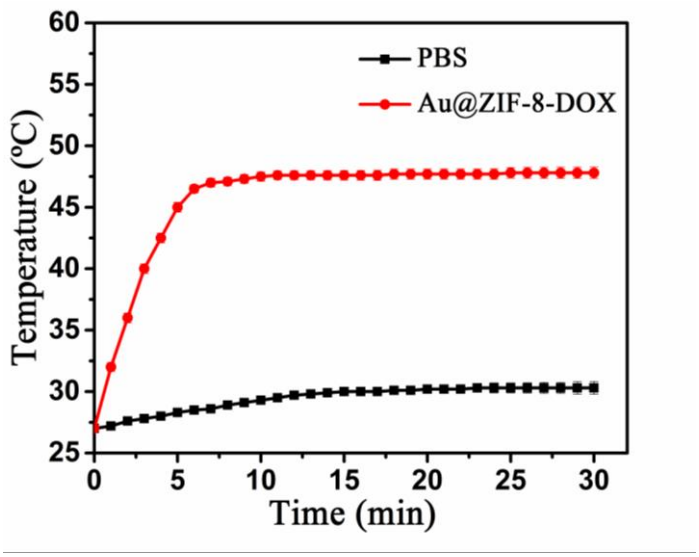

Fig. S6 The temperature change of Au@ZIF-8-DOX complexes in PBS buffer solutions with laser irradiation (wavelength of 514 nm and intensity of 50 mW). Pure PBS solution (pH = 7.4) was used as negative control.

The temperature of Au@ZIF-8-DOX complexes in PBS buffer solutions can be rapidly increased from 27°C to 47°C within 6 min laser irradiation, demonstrating the photothermal effect of Au@ZIF-8-DOX complexes.

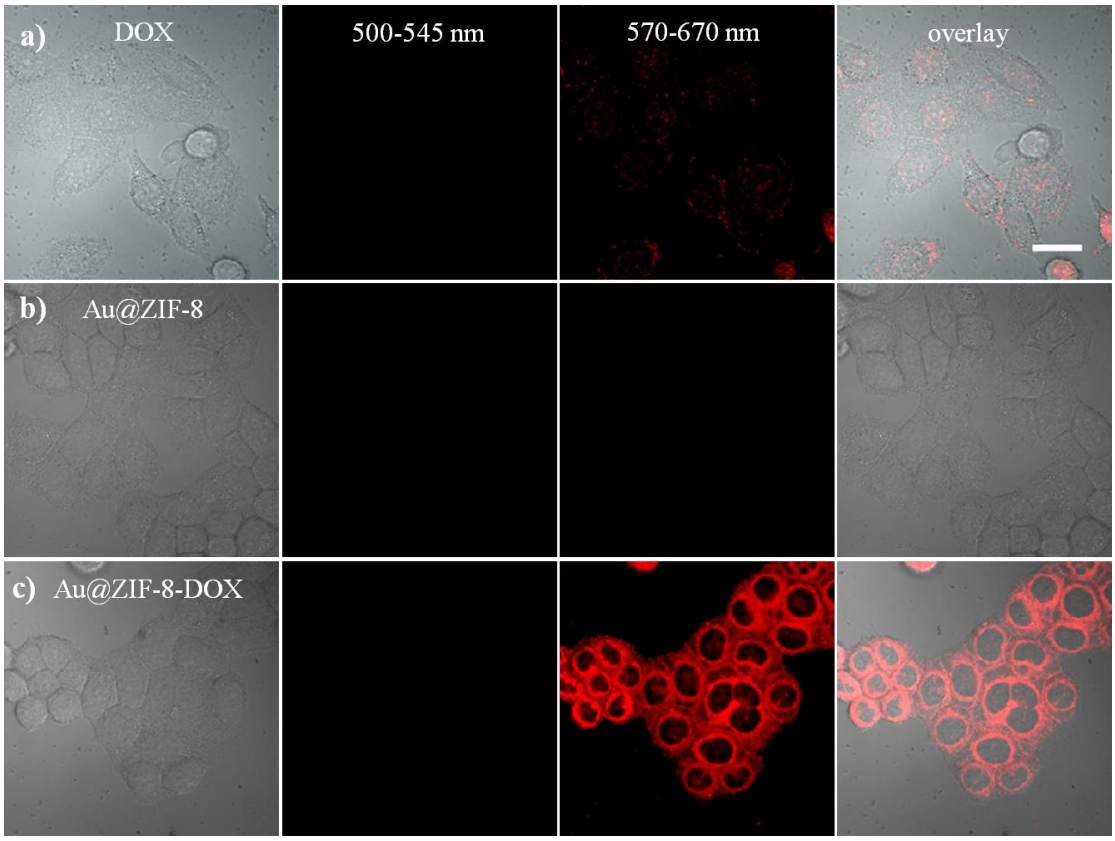

Fig. S7 Intracellular localization of (a) DOX, (b) Au@ZIF-8 and (c) Au@ZIF-8-DOX with organelle-specific probes including Lyso-Tracker Red using confocal microscope. Scale bar: 20 μm. Column 1: bright images; Column 2: images observed during the 500 - 545 nm; Column 3: images observed during the 570 - 670 nm; Column 4: overlay images.

Seen from Fig. S7, it is obvious that no fluorescence is observed for the HeLa cells incubated by the Au@ZIF-8 nanostructures. On the contrary, after the HeLa cells are incubated by the Au@ZIF-8-DOX complexes, obvious red florescence can be observed owing to the florescence property of DOX, illustrating that the Au@ZIF-8-DOX complexes can be easily localized in the cytoplasm of the HeLa cells.

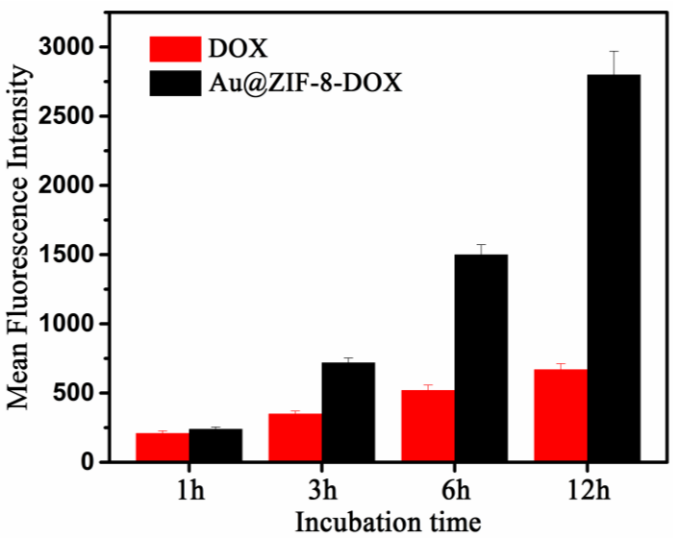

Fig. S8 Cellular uptake of free DOX and Au@ZIF-8–DOX complexes quantified by flow cytometry.

The Au@ZIF-8-DOX complexes exhibited higher cellular uptake than free DOX.

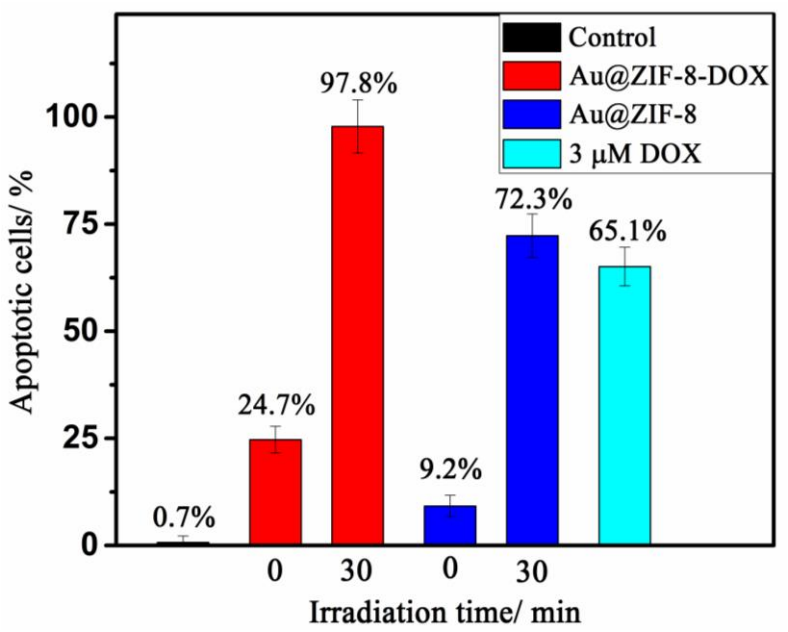

Fig. S9 Comparison of apoptosis rate of Au@ZIF-8-DOX-treated and Au@ZIF-8-treated (10 μM equivalent DOX) HeLa cells, which are irradiated by a 20 $mW \cdot cm^{-2}$ light with the wavelength of 400-700 nm for different minutes, respectively, and then replaced with culture medium and cultivated for 24 h at 37°C in the dark. The HeLa cell apoptosis rate is determined by flow cytometry.

Part SIII: Evaluation of loading ability of core-shell Au@ZIF-8 nanostructures toward DOX.

Table S1 DOX loading content and entrapment efficiency of core-shell Au@ZIF-8 nanostructures.

Au@ZIF-8 concentration (mg/mL)	DOX concentration (mg/mL)	Loading Content (%)	Entrapment Efficiency (%)
0.400	0.100	41.05	69.65
0.400	0.200	44.25	79.38
0.400	0.400	46.65	87.43
0.400	0.600	47.48	90.41
0.400	0.800	47.40	90.11

Seen from Table S1, a series of concentration of DOX (from 0.1 to 1.0 mg/mL) was explored. Notably, as the DOX concentration is increased to 0.6 mg/mL, the loading content could be up to 47.48% and correspondingly the entrapment efficiency can achieve 90.41%. Unfortunately, when the DOX concentration continues to increase (>0.6 mg/mL), the DOX loading content and entrapment efficiency could not go up further.

The drug loading content and the entrapment efficiency in Table S1 are obtained with the following equations.

$$Loading\ \ content = \frac{weight\ of\ \ drug\ \ in\ \ Au@ZIF-8}{weight\ of\ \ Au@ZIF-8-DOX}$$

$$Entrapment\ efficiency = \frac{weight\ of\ \ drug\ \ in\ \ Au@ZIF-8}{initial\ \ weight\ of\ \ drug}$$

In the equations, initiate weight of drug, weight of drug in Au@ZIF-8 and weight of Au@ZIF-8-DOX are listed in Table S2.

Table S2 Experimental results needed for calculating the loading content and the entrapment efficiency.

Initial weight of drug (μg)	Weight of drug in Au@ZIF-8 (μg)	Total weight of Au@ZIF-8-DOX (μg)	Loading Content (%)	Entrapment Efficiency (%)
500	348.23	848.23	41.05	69.65
1000	793.84	1793.84	44.25	79.38
2000	1748.50	3748.50	46.65	87.43
3000	2712.24	5712.24	47.48	90.41

In Table S2, the embedded DOX weight in the Au@ZIF-8 nanostructures is estimated by subtracting the concentration of the DOX in the supernatal solution after mixture from the initiate concentration of DOX before mixture. And the DOX concentration in the solutions is calculated by the equation (y = 0.01103x + 0.00526) in Fig. S10, in which the absorption intensity is measured at 480 nm by UV-Vis spectra.

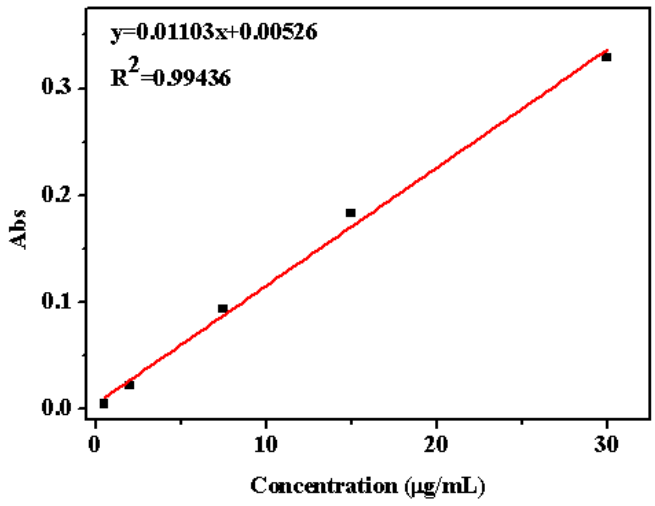

Fig. S10 Standard curve of DOX in aqueous solution.